LHCB-2003-83
EXPT
22nd September 2003

Radiation background in the LHCb experiment.

G.Corti
CERN, Genève

L.Shekhtman
Budker Institute of Nuclear Physics, Novosibirsk

Abstract

In this note we present results of simulations studies on radiation background for the whole LHCb experimental setup. Particle fluences, their energy spectra and absorbed doses along the detector and in the various subsytems, in particular for some critical areas where the electronics is envisioned to be located, are shown.

1 Introduction

The knowledge of particle fluences, their energy spectra and absorbed doses is a crucial ingredient to properly estimate the damage probability of detectors and electronics. Several types of damage can be distinguished togheter with the different types of particles and processes that are responsible. Some damages are gradual effects taking place during the whole lifetime of the devices exposed to radiation, others are due to the energy deposited by a single particle and as such have a certain probability of occurence that depends on the sensitivity of the devices.

Total ionizing dose is a cumulative effect produced by energy deposition of charged particles passing through a device. In the interface regions of semiconductor devices (insulator layers, contacts, etc.) this leads to accumulation of space charge that distorts the electric field and can produce micro-discharges leading to the degradation of the devices. Another gradual effect produced by neutrons and charged hadrons is displacement damage of Silicon lattice by Non Ionizing Energy Loss (NIEL). This process depends on the particle fluence and takes place in the whole bulk of a Silicon device leading to the increase of dark current and depletion voltage.

High energy hadrons interacting with the material of the electronics can produce very strong local ionization. This strong local charge collection can upset the content of a memory cell and revert individual triggers or switches (Single Event Upset, SEU) or even cause the permanent damage of devices (Single Event Latch-up, SEL). To evaluate the probabilty of such events occuring is necessary to know the energy distribution and fluence of the various type of particles to convolute it with the specific sensitivities of the devices.

Radiation background in different regions of the LHCb experiment has been studied in the past with different detector layouts, where variations of the Technical Proposal design with more realistic descriptions of detector elements as available at the time of the studies were introduced. Radiation levels and fluxes were obtained for the VELO [1], Calorimeters [2] and Silicon Trackers [3] with the MARS IHEP program. In addition detailed studies of background in the muon system have been perfomed with GCALOR [4] [5].

Studies have ben recently performed with simulations based on FLUKA [6] for various locations in the re-optimized LHCb detector layout. A review of the results obtained is presented in this note. Fluences for e^+/e^-, neutrons and charged hadrons, as well as maps of the absorbed dose levels in the overall experiment and in specific places for all subsystems have been obtained. Particle spectra have also been produced in a number of locations, usually corresponding to the same position where integral fluences were recorded. The complete set of simulation results of which a subset is presented here, is available elsewhere [7].

All results are given in units normalized per one p-p collision. In order to calculate a corresponding value per second the results can be multiplied by a given factor that depends on the running luminosity of the experiment. For the nominal LHCb average luminosity of $2 * 10^{32} cm^2 s^{-1}$ this factor is $1.6 * 10^7$ collisions per second and $1.6 * 10^{14}$ collisions per LHC-year (10^7 seconds).

2 Simulation Conditions

The results were obtained with simulation of the whole LHCb experiment with the FLUKA package, as mentioned in the Introduction. The LHCb re-optimized layout [8] was described, and the latest available geometry of the different detectors and infrastructures used. An exception is the Trigger Tracker station located before the magnet where a combination Inner-Outer trackers was still used[1]. A vertical cross section (x=0) of the overall geometry as modelled in the FLUKA simulation is shown in Fig. 1. The whole layout of the experiment can be seen as well as the cavern. The various subsytems can be seen with, from left to right, the Vertex Locator (VELO), RICH1, the Trigger Tracker (TT), the main dipole magnet, the downstream tracking stations (T1-T3), RICH2, the Calorimeters, the Muon System and the beam pipe crossing the whole detector. A preliminary design of a tunnel under RICH2 was introduced. Details regarding the different subsystems are described in each of the following subsections where the corresponding results are presented.

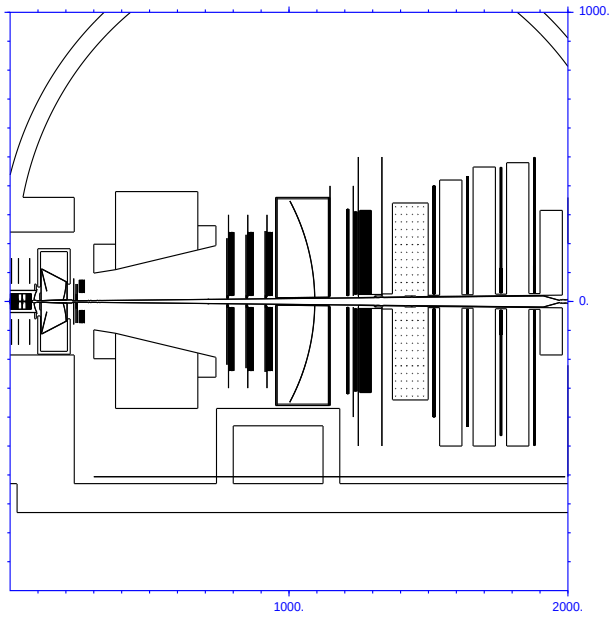

Figure 1: Cross section (at x=0) of the LHCb FLUKA model including the experimental hall. All subsystems can be seen from left to right

The thin lines that can be seen in the figure close to the detectors are some of the scoring planes where the radiation distributions were recorded. It can be noted that one plane was located just above the floor of the cavern.

The following energy thresholds were used in the simulations for particles transport:

- 1 MeV for electrons and positrons,
- 0.1 MeV for photons,

[1]The FLUKA model was based on what described in SICBMC v249 (the GEANT3 based simulation of LHCb) except for the beam pipe and the magnetic field that are later versions (pipe v9.0, field 4.3).

- 10^{-11} MeV for neutrons,
- 50 MeV for anti-neutrons
- 0.1 MeV for other particles.

Primary events were generated with the DPMJET-II program [9]. The results shown are based on the equivalent of about 35000 p-p collisions.

3 Simulation results

An overview of the radiation background in the whole LHCb is shown in Fig.2-5, where the fluences of neutrons, e^+/e^-, charged hadrons and the dose map are shown in a cross section of the experiment along the vertical plane x=0.

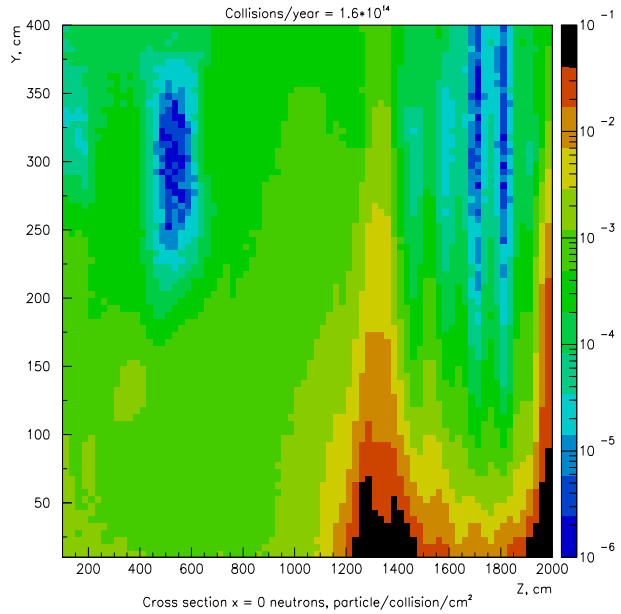

Figure 2: Neutron fluence for a cross section ($x = 0$) of the whole experiment

It can be noted in Fig.2 that the main source of neutrons in the experiment is the inner parts of the electromagnetic and hadron calorimeters between 1200 and 1500 cm in z. Primary particles interact with the material in this regions and hadronic showers start developing producing a strong flow of neutrons. In the region of the Tracker stations the neutrons flow is significantly reduced due to the distance from the source and the absorption of the showers in the material of the Calorimeters and the other detectors in between. As a result the neutrons fluence in the Trackers regions becomes almost uniform in y-z with quite moderate values between 10^{-4} and 10^{-3} particles/cm^2/collision.

Other sources of neutrons are the separation dipole magnets located downstream of the Muon system and upstream of the VELO (respectively at about 20 and -3 m from the Interaction Point). Neutrons from the downstream separation dipole are stopped by the Muon shields and affect mainly the inner parts of the last Muon stations (M5 and M4).

Background from the upstream separation dipole can be reduced by a proper choice of shielding in the tunnel between the magnet and the VELO tank. A shielding has been introduced in the simulation as discussed later in VELO subsection.

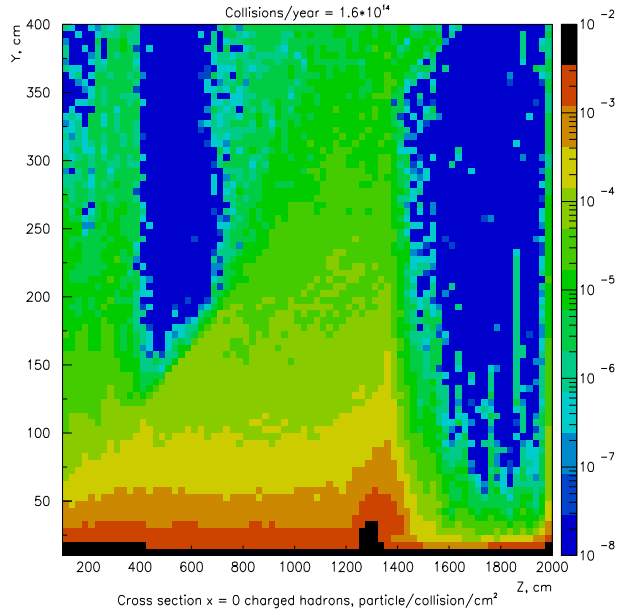

Figure 3: Charged hadrons fluence for a cross section ($x = 0$) of the whole experiment

Charged hadrons in the whole detector from the VELO to the Calorimeter region originate mainly from the primary interactions. As a result, their fluence distribution in the experiment is non uniform in x-y and strongly peaked toward the beam axis as can be seen in Fig.3.

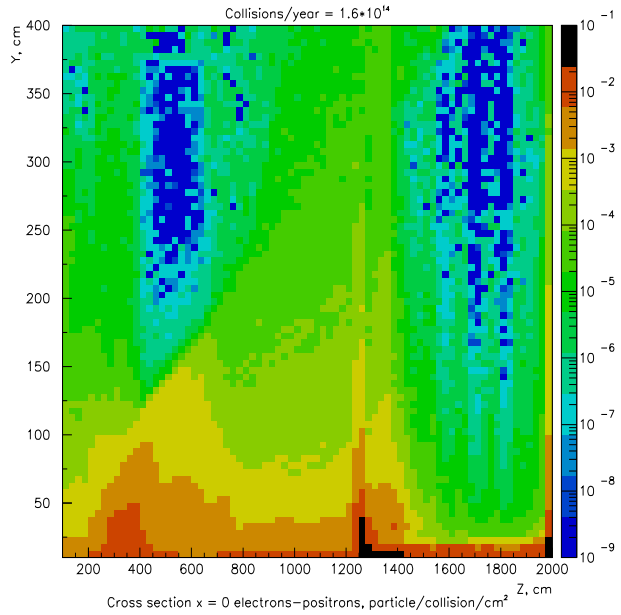

Figure 4: Electron-positron fluence for a cross section ($x = 0$) of the whole experiment

In addition the x and y distribution behind the magnet reflect the effect of the LHCb dipole magnetic field. Behind the calorimeters the charged hadrons are almost completely stopped by the muon shields. Most of the electrons and positrons in the experiment are produced in electromagnetic showers along the beam pipe and in the Calorimeters. In Fig.4 a clear peak of electron-positron fluence can be observed at the entrance of the main dipole magnet (z$\sim$300 cm) where low momentum electrons, produced in the flanges of the beam pipe, are curling.

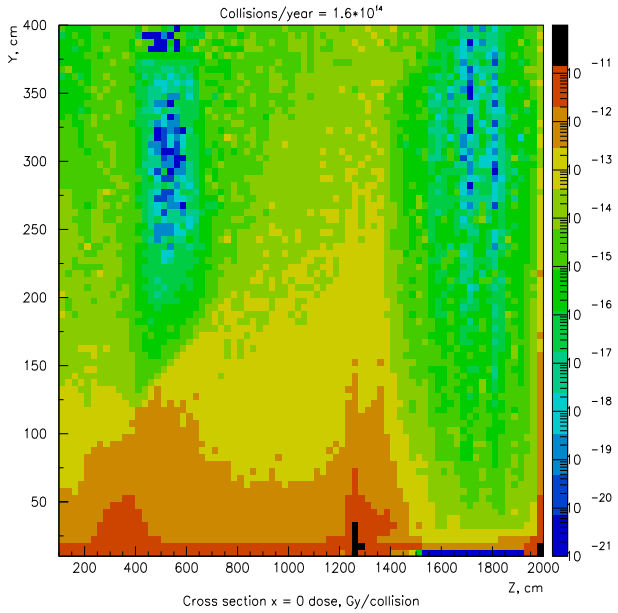

Figure 5: Dose for a cross-section ($x = 0$) of the whole experiment

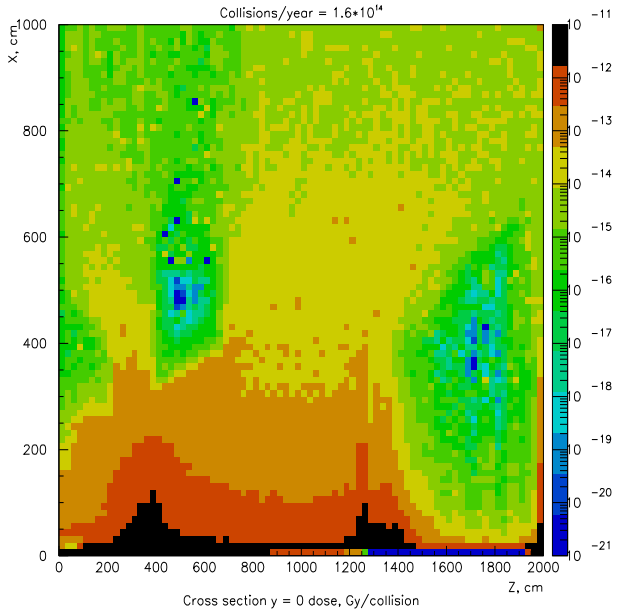

Figure 6: Dose map in the cross section plane $y = 0$

Since ionization dose is deposited by charged particles it has its maxima in the regions where electromagnetic and hadronic showers are produced. The two main locations where this occurs are at the entrance of the main dipole magnet, where electromagnetic showers appear mostly from the flanges of the beam pipe and at the entrance of the calorimeters. It can be seen in Fig. 5 that the dose is also high in the vertex region close to the interaction point and along the beam line where the flux of primary particles is higher.

The dose map along a cross section plane y=0 is shown in Fig. 6 while the dose map along the floor of the cavern can be seen in Fig. 7.

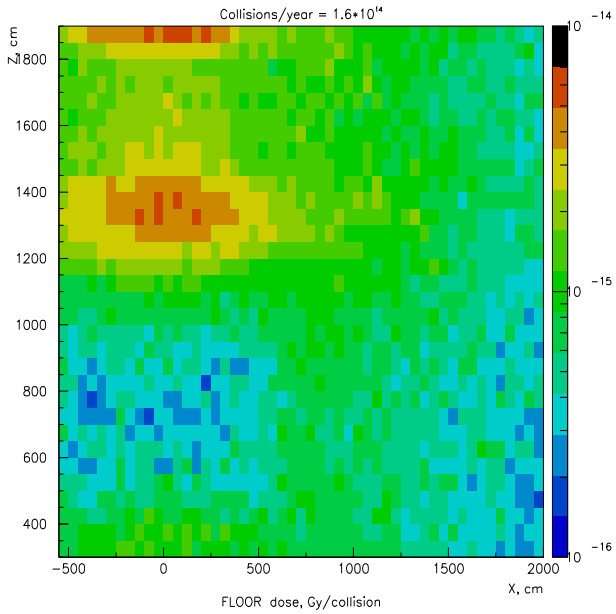

Figure 7: Dose map along the floor of the cavern (y=-600cm)

The minimum value of the dose on the cavern floor is in the concrete tunnel introduced below RICH2. In this location the dose is around $3.6 * 10^{-14}$ Rad/collision (60 Rad/10 LHC-years). Another place on the cavern floor where there are lower dose values is the area at x $>$ 10m and z $<$ 10m with values smaller than $5.6 * 10^{-14}$ Rad/collision (90 Rad/10 LHC-years).

Particle energy spectra in the Inner Tracker of Tracker station 1 are shown in Fig.8 as an example. The neutrons energy distribution looks as a regular "spallation" spectrum, with its maximum around 1 MeV, a sharp cut-off at high energies and a long tail down to thermal neutrons energies. Neutrons with kinetic energy higher than 0.1 MeV give a substantial contribution to many of the damaging effects in electronics devices. Pions constitute almost the whole of the charged hadrons at high energy while at low energies some contribution of protons is observed. Low-momentum protons can contribute quite significantly to the NIEL and produce bulk damage in silicon. The electrons spectrum extends towards low energies where a cut-off due to the transport threshold of the simulation is present. Electrons contribute mainly to the ionization dose and their contribution to other damaging effects is negligible.

In order to estimate bulk damage effect in Silicon from the radiation background, we

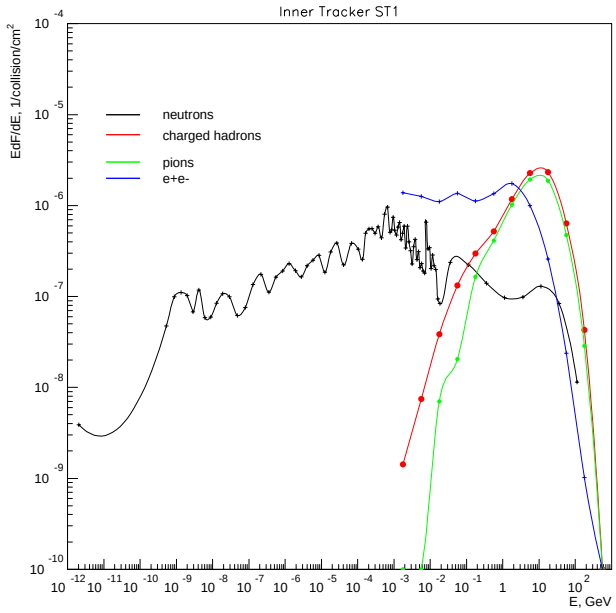

Figure 8: Energy spectra at the Inner Tracker of T1 ($z = 783$ cm)

calculated the 1 MeV neutron equivalent fluences (for Silicon) by convoluting the spectra with available NIEL cross sections [10].

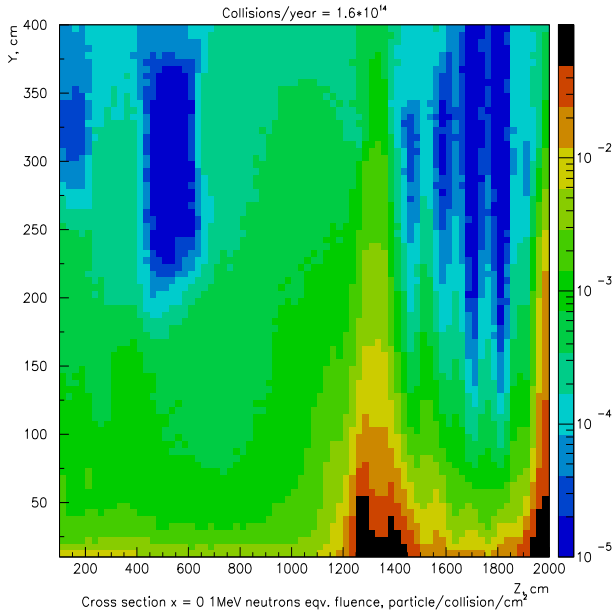

Figure 9: 1-MeV neutron equivalent fluence, cross-section of the experiment at X=0.

The map of 1 MeV neutron equivalent fluence in the whole experiment for the cross section plane x=0 is shown in Fig. 9. Close to the beam line where the density of charged hadrons is higher the 1 MeV neutron equivalent fluence is mostly determined by charged hadrons as can be noted comparing Fig. . 9 with Fig. 3. In the regions with high neutron

fluence and far from the beam line the 1-MeV n-equivalent fluence is instead dominated by neutrons as can be seen comparing with Fig. 2.

Results relative to the different subsystems are reported in the following subsections.

3.1 VELO

A vertical cross section of the simulation model of the region around the interaction point is shown in Fig. 10. The dipole magnet and the shielding wall inside the tunnel, the VELO tank and sensitive stations around the interaction point, and RICH1 with its iron magnet shield around the photo-detectors at the opening of the tunnel can be seen from left to right.

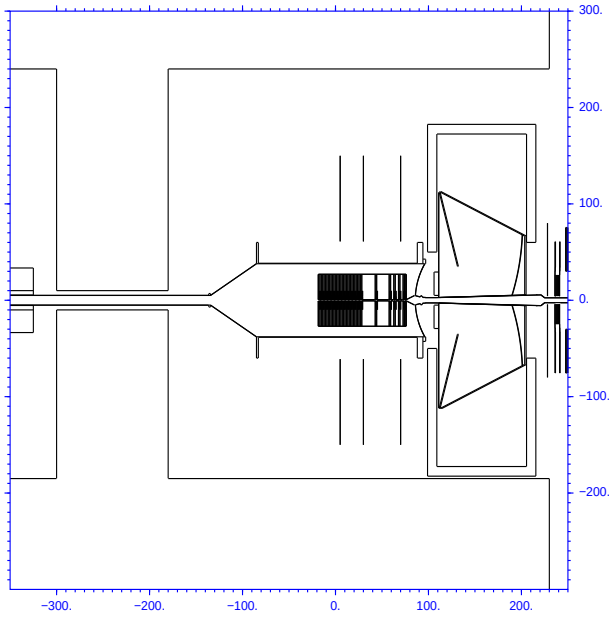

Figure 10: Geometrical model of the vertex region

A concrete shielding wall between the separation dipole and the interaction point was introduced to reduce the neutron background from the dipole due to interactions of primary particles with the material of the magnet, as shown in the figure. Although such a shield is foreseen no technical design was available and a 1 m thick concrete wall with a 20 cm diameter hole around the beam pipe was chosen after a very brief optimization.

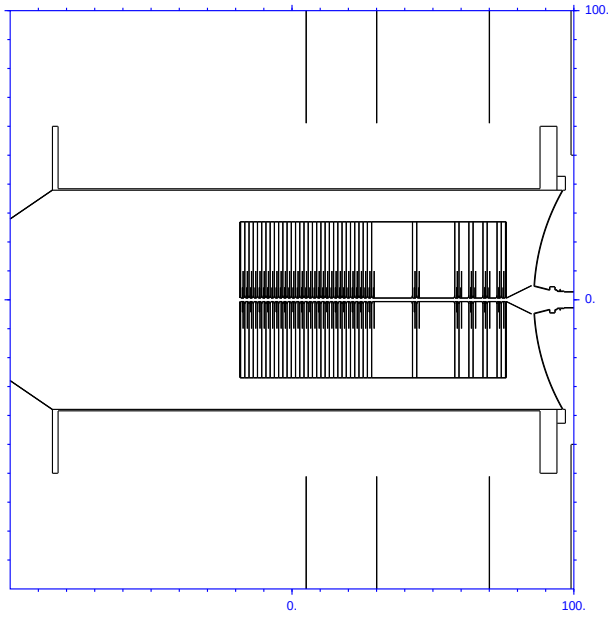

Figure 11: Closer view of the VELO geometrical model

A closer view of the VELO is shown in Fig. 11. It includes the Silicon sensors, the RF shield with configuration and dimensions as optimized for the VELO TDR [11], and 1 mm thick carbon fiber supports, 20 cm high and extending to the walls of the tank. The present model does not contain any additional details inside or outside the VELO tank. The thin vertical lines above and below the tank are scoring planes.

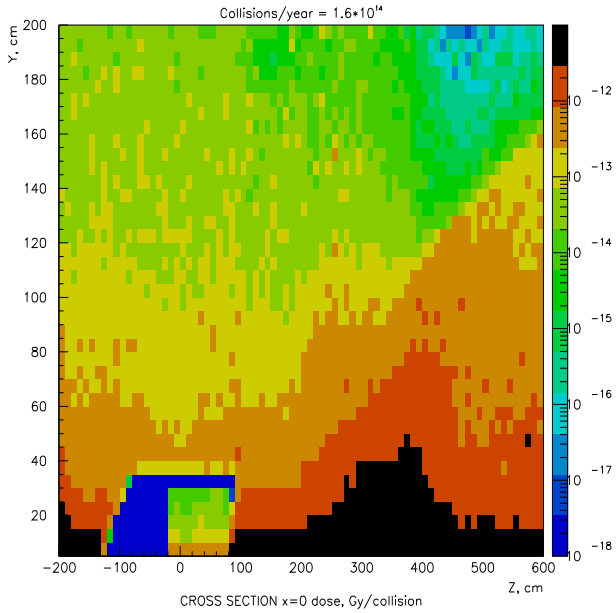

Figure 12: Dose map in the vertex region (cross section plane x=0)

The dose map and 1 Mev n-equivalent fluence in the VELO region for the cross-section plane x=0 are shown in Fig. 12 and Fig. 13 respectively.

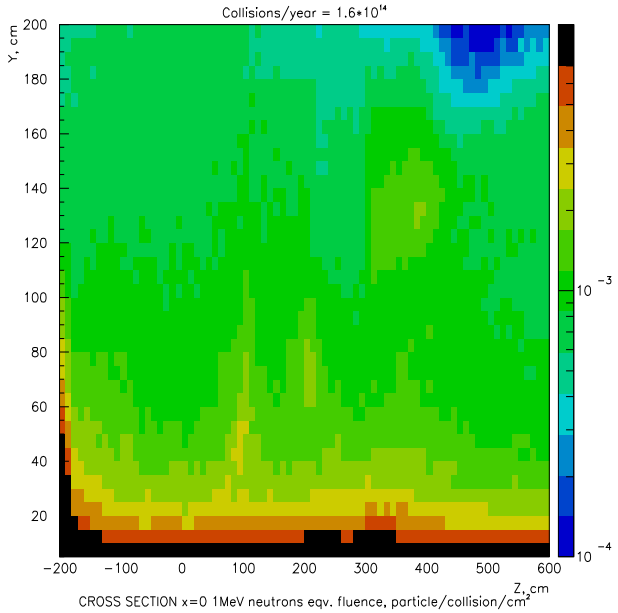

Figure 13: Map of 1-Mev n-equivalent fluence at the vertex region (cross section plane x=0)

The maximum value of the dose level in the material of the Si sensors is close to the beam axis. The dose at inner edge of a sensor is as high as $3.1 * 10^{-8}$ Rad/collision (50 MRad/10 LHC-years) as can be can seen in Fig. 14, where the dose map for the most downstream silicon sensor (Z=73cm) is shown. In the tunnel around the VELO the dose maximum value is about $2.3 * 10^{-11}$ Rad/collision (37 kRad/10 LHC-years) at the surface of the tank, dropping down to $5 * 10^{-12}$ Rad/collision (8 kRad/10 LHC-years) at a distance of 1 m from the VELO tank.

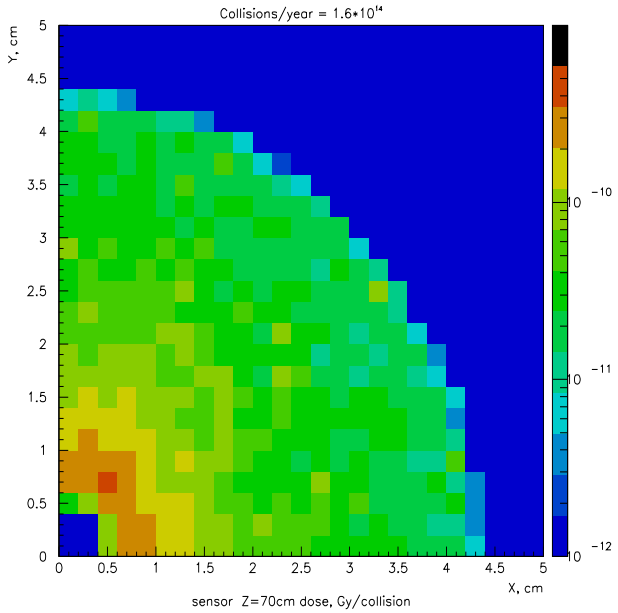

Figure 14: Dose map at the most downstream VELO station (z=73cm)

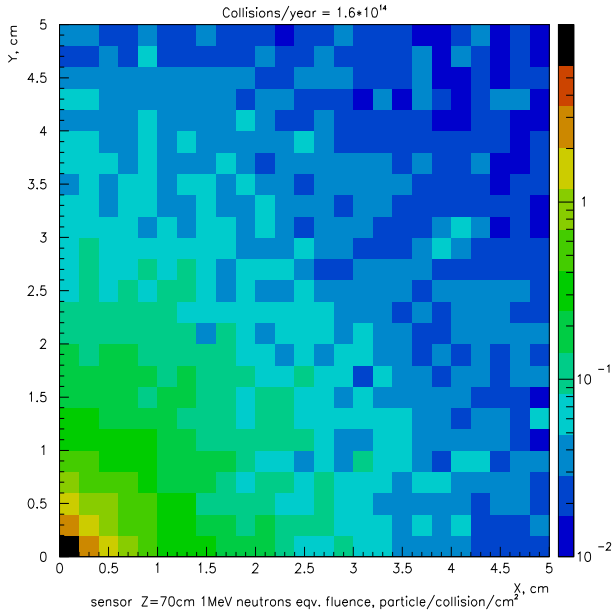

Figure 15: 1-MeV equivalent fluence at the most downstream VELO station (z=73cm)

The 1 MeV n-equivalent fluence inside the VELO tank is dominated by primary charged hadrons. The value of n-equivalent fluence for the inner edge of the sensor is as high as 1.5 n/cm^2/collision ($2.4 * 10^{15}$ n/cm^2/10 LHC-years), as shown in Fig. 15, while in the tunnel near the VELO tank the value of 1 MeV n-equivalent fluence is about $1.3 * 10^{-3}$ n/cm^2/collision ($2.0 * 10^{12}$ n/cm^2/10 LHC-years).

3.2 Trackers

A cross section of the LHCb FLUKA model for the plane x=0 in the Trackers region is shown in Fig.16. From left to the right one can see TT, the main dipole magnet and the downstream stations T1, T2 and T3. The TT station design was kept as a combination Inner/Outer tracker, as the final design of TT was not available when the simulation model for these high statistic studies was frozen. Each tracking station consists of an outer and inner part. The Outer Tracker (OT) stations are modelled by combining the different layers in the z-direction to represent an average structure of the straw-tubes and supports. OT frames are not included in the model.

In the TT region, just before the main dipole magnet, a significant contribution to the dose comes from electrons-positrons produced in the showers in the flanges of the beam pipe and curling near the entrance to the magnet. In the most inner part, closer to the beam line, the dose is mainly due to primary particles. The x-y dose distribution in a plane at z = 228 cm (upstream of TT) is shown in Fig. 17. At the surface of the vacuum pipe wall at x = 4cm, y = 0 the dose reaches $3*10^{-9}$ Rad/collision (4.8 MRad/10 LHC-years) dropping to $8 * 10^{-11}$ Rad/collision (130 kRad/10 LHC-years) at x = 50 cm, y = 0 and $5 * 10^{-11}$ Rad/collision (80 kRad/10 LHC-years) at x = 0, y = 50cm.

The 1 MeV n-equivalent fluence in the TT region is produced by primary particles in the inner part close to the beam line and by neutron fluence from the vertex tunnel at

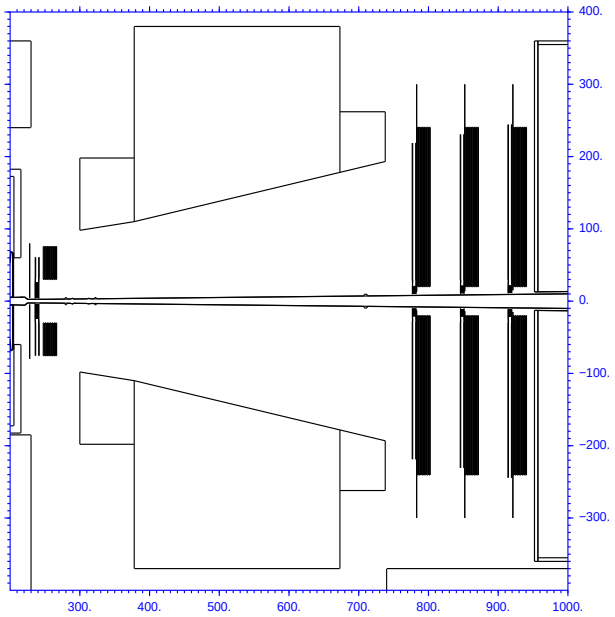

Figure 16: Cross section (x=0 plane) of the LHCb FLUKA model of the Trackers region

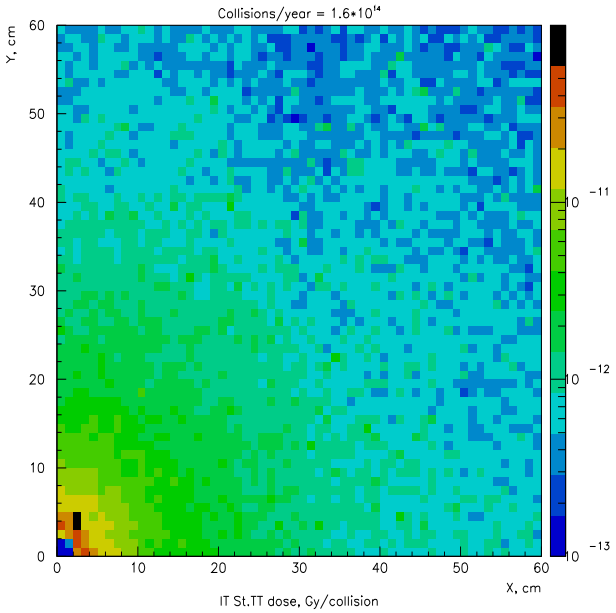

Figure 17: Dose distribution at a cross section plane in the region of the Trigger Tracker (z=228 cm)

the larger radius ($>$ 50cm). The distribution of 1 MeV n-equivalent fluence in the z = 228 cm plane is shown in Fig. 18. Close to the surface of the beam pipe (x=4cm, y=0) 1 MeV n-equivalent fluence is around $3 * 10^{-2} n/collision/cm^2$ ($4.8 * 10^{13} n/cm^2/10 LHC - years$). At x=50cm, y=0 n-equivalent fluence drops down to $10^{-3} n/collision/cm^2$ ($1.6 * 10^{12} n/cm^2/10 LHC - years$).

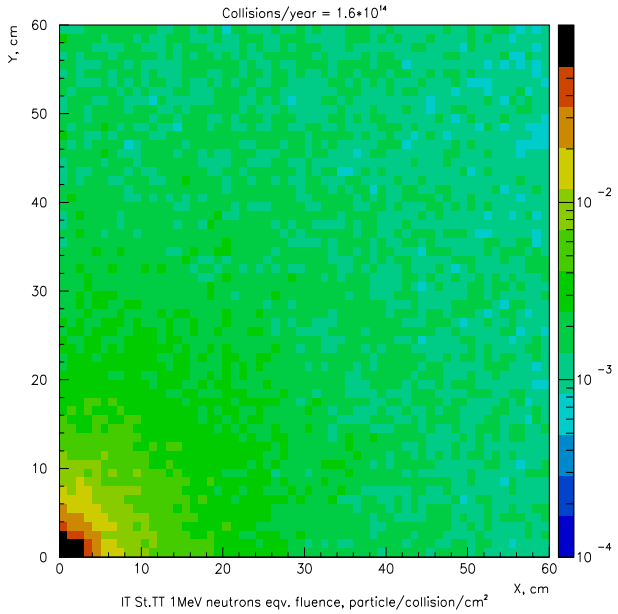

Figure 18: Distribution of 1 MeV n-equivalent fluence for Si in a cross section plane in the TT region (z=228cm)

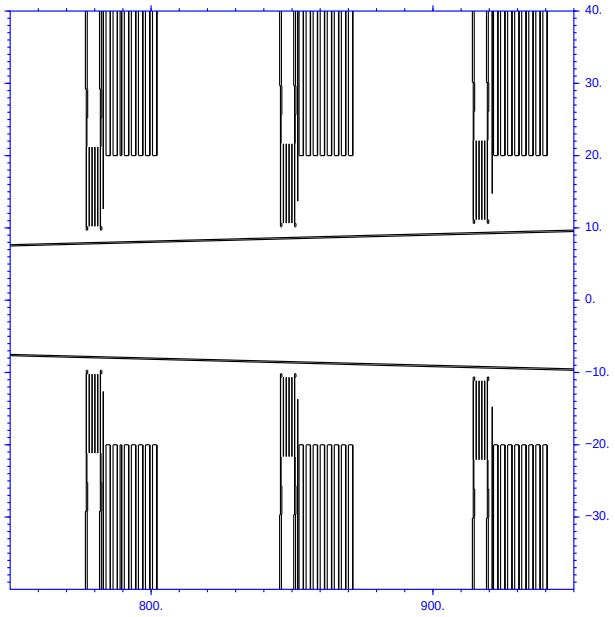

Figure 19: Cross section (x=0 plane) of the FLUKA model of the Trackers, with a closer view of the IT downstream stations (y and z are in different scales)

A closer view of the Inner Tracker(IT) stations of the downstream Trackers is shown in Fig. 19. The IT cross-shaped layout [12] is described in the geometrical model implemented in FLUKA; the boxes, close to the beam pipe, containing each 4 sensor planes can be seen in the Figure. Downstream of each box the corresponding OT stations layers are also visible.

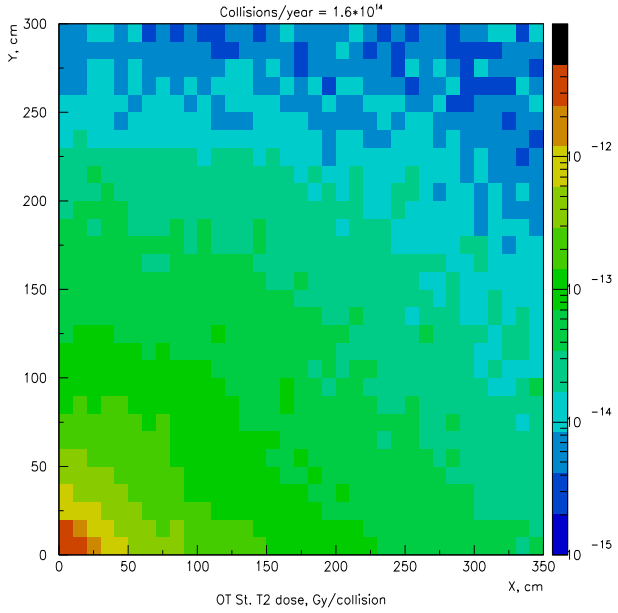

Figure 20: Dose in T2 (x-y plane) at $z = 852$ cm

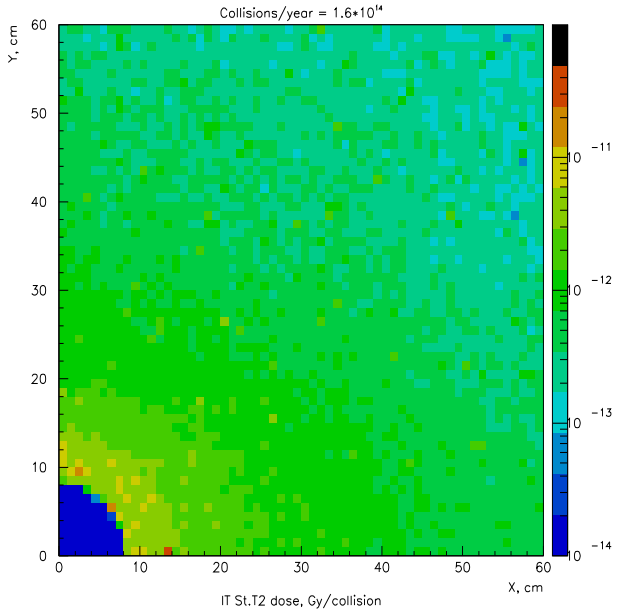

Figure 21: Dose in IT region of T2 (x-y plane) at $z = 852$ cm

In the Trackers region the contributions to the dose come from the fluences of charged hadrons and electrons-positrons. The dose level does not change much from T1 ($z \sim 780$

cm) to T3 (z *sim* 920 cm) as can be seen in Fig. 5. Detailed dose distributions in the x-y plane have been obtained for all trackers. The x-y distributions for T2 are shown in Fig. 20 for the full surface and in Fig. 21 where a zoom of the IT region is shown. In the left bottom corner of this second figure one can see the vacuum pipe inside which no dose was recorded. The dose distributions are only slightly asymmetric in the x-y plane with higher values towards the x-axis, as low-momentum particles (mostly e^+/e^-) curved by the magnetic field, and higher-momentum charged hadrons almost equally contribute to it. The dose varies from about $6.3 * 10^{-10}$ Rad/collision ($\sim$ 1MRad/10 LHC-years) at x=9 cm (closest to the beam line) to around $6.3 * 10^{-11}$ Rad/collision ($\sim$ 100 kRad/10 LHC-years) at x=50 cm and to about $1.3 * 10^{-12}$ Rad/collision (2.1 kRad/10 LHC-years) at the outer edge of the OT station (x=290cm).

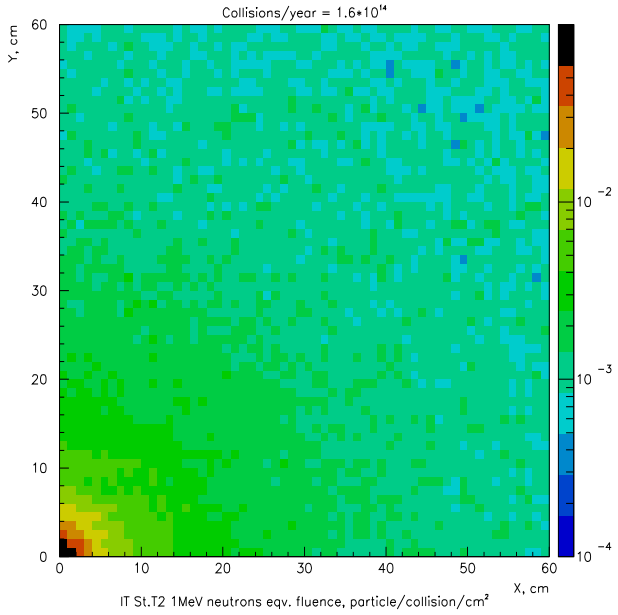

Figure 22: 1 Mev neutron equivalent fluence in IT region of T2 (x-y plane) at $z = 852$ cm

The map of the 1 MeV n-equivalent fluence for Silicon in the Inner Tracker region of T2 in the x-y plane is shown in Fig. 22. At small radius the 1 MeV n-equivalent fluence is mainly determined by charged hadrons. On the other hand far from the beam line, where the charged hadrons fluence is low, the main contribution to the 1 MeV n-equivalent fluence is given by neutrons and the distribution is more uniform. As seen in the figure, the value of the 1 MeV n-equivalent fluence varies from $5.6*10^{-3}$ n/cm^2/collision ($9*10^{12}$ n/cm^2/10 LHC-years) at x = 10 cm, to $1.3*10^{-3}$ n/cm^2/collision ($2*10^{12}$ n/cm^2/10 LHC-years) at x = 50 cm.

A detailed review of simulation results obtained for the Inner Trackers with the same simulation setup but lower statistic is available [13] as well as distributions for all Trackers as obtained with the high statistic studies reviewed in this note [7].

3.3 RICHes

3.3.1 RICH1

A close vertical view of the RICH1 simulation model is shown in Fig.23 (x=0). The main feature affecting the background around this subsystem is the iron magnetic shielding box of the photo-detectors.

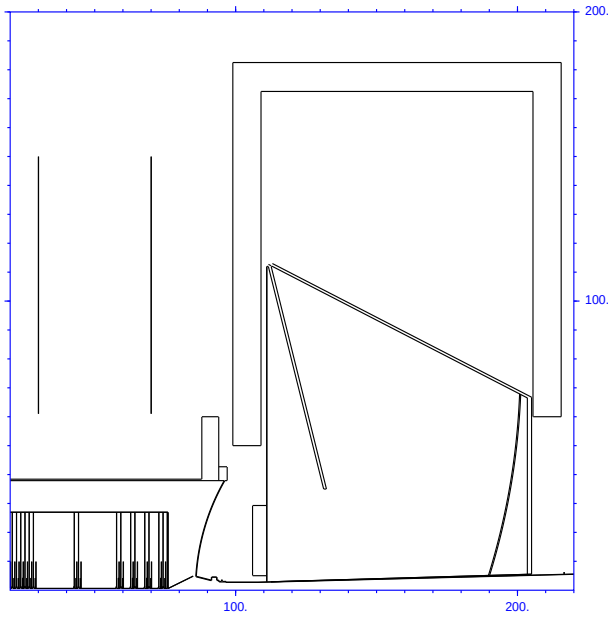

Figure 23: Simulation model of RICH1 ($x = 0$ plane)

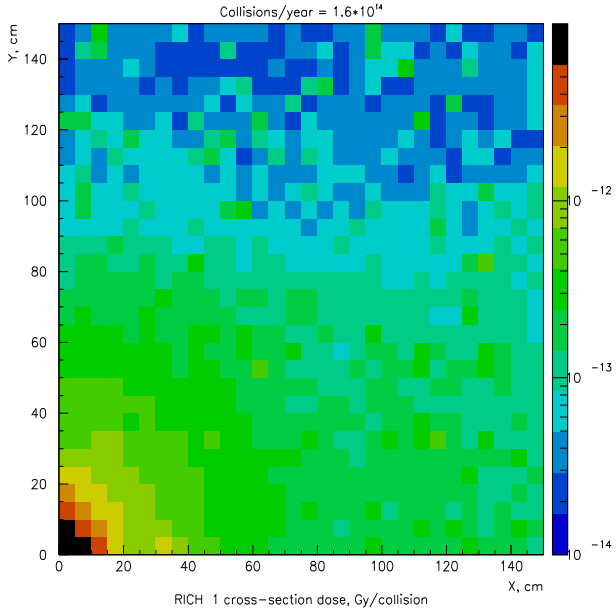

Figure 24: Dose in RICH1 in an x-y cross section plane at $z = 160$ cm

The dose and 1 MeV n-equivalent fluence maps are shown in Fig. 24 and 25 in an x-y cross section plane in the middle of RICH1 (z=160cm). The dose value is significantly reduced inside the magnetic shielding box where the photo-detectors and their electronics are located (y $\gtrsim$ 80 cm). The dose values in this area are less than $7.5{*}10^{-12}$ Rad/collision (12 kRad/10 LHC-years) and the 1 MeV n-equivalent $1.1{*}10^{-3}$ n/cm^2/collision ($1.7{*}10^{12}$ n/cm^2/10 LHC-years).

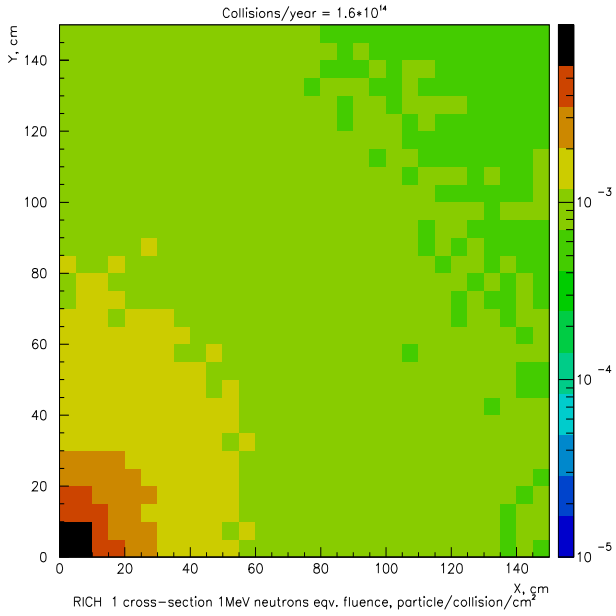

Figure 25: 1-MeV n-equivalent fluence at the cross-section of RICH1 at $Z = 160$ cm.

3.3.2 RICH2

In Fig. 26 a cross section (in the x=0 plane) of the RICH2 simulation model is shown. The photo-detectors (outside the LHCb acceptance) have not been introduced.

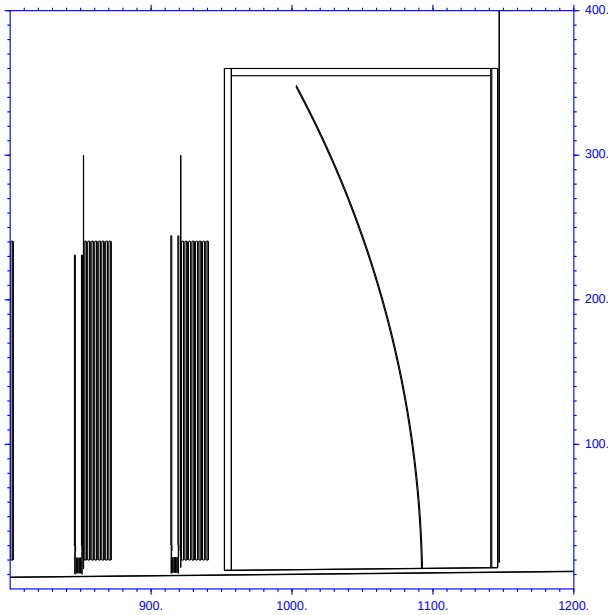

Figure 26: Cross section of the RICH2 simulation model ($x = 0$ plane)

The dose map in a 700 μm Silicon x-y plane located just downstream of RICH2 (at z=1147cm) is shown in Fig. 27. Electronics could be located at the outer edges of RICH2: in this area the maxima of the dose are along the axis at x=4m, y=0 and at x=0, y=3m with values of $2.7 * 10^{-12}$ Rad/collision (4.3 kRad/10 LHC-years) and $1.5 * 10^{-12}$ Rad/collision (2.4 kRad/10 LHC-years) respectively

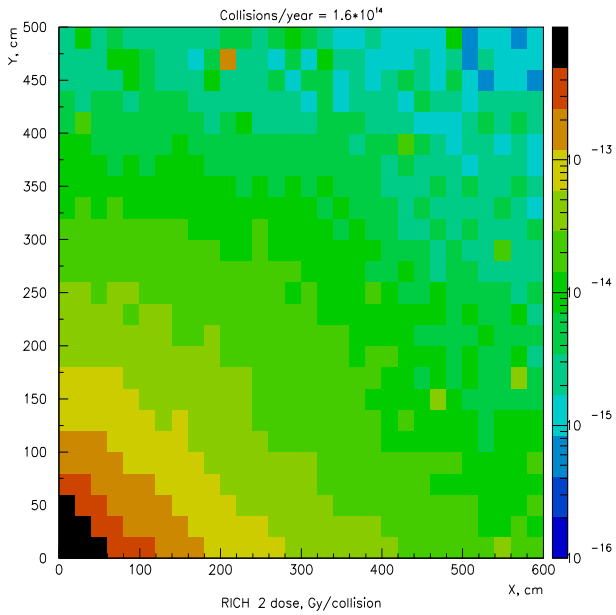

Figure 27: Dose in a plane downstream of RICH2 at $x = 1147$ cm

3.4 Calorimeters.

3.4.1 Preshower and Electromagnetic calorimeter.

The Preshower and the Electromagnetic Calorimeter (ECAL) are shown in Fig. 28 in a x=0 cross section plane. Both subsystems were modeled in the FLUKA simulation with a simplified structure, in the z direction, of the sensitive and converter material layers as can be seen in the drawing. The structure and material of the layers were taken from corresponding technical notes [14], [15]. The most upstream detector in the figure is the first Muon station M1.

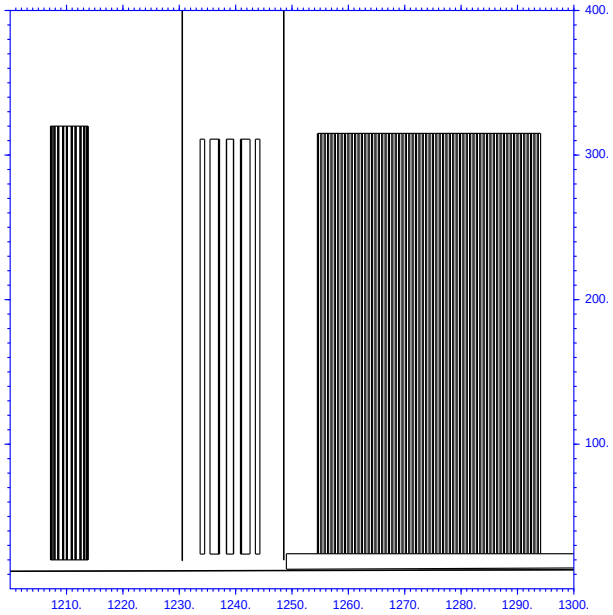

Figure 28: The Preshower and ECAL as seen in a $x = 0$ cross section

The dose maps recorded in two x-y planes just in front of the Preshower and of ECAL (the two thin lines in Fig. 28) are shown in Fig. 29 and 30. Maximum values of the dose are reached at the inner edges of the Preshower and of ECAL where an iron shield protecting the Muon stations 2-5 is located ("Calorimeter Plug"). Most of the very forward primary particle just outside of the beam pipe are stopped by this plug initiating showers and producing a major part of the radiation background in the experiment. Dose values at the inner edges of the Preshower and ECAL (x = 0, y = 30 cm, z = 1230 cm and 1250 cm) are around $1.8 * 10^{-10}$ Rad/collision (290 kRad/10 LHC-years) and $8.2 * 10^{-10}$ Rad/collision (1.3 MRad/10 LHC-years) respectively.

A possible location of the electronics for both Preshower and ECAL is on top of the detectors. For the Preshower the dose values in this area are about $1.2 * 10^{-12}$ Rad/collision (1.9 kRad/10 LHC-years) in the center (x=0, y=3.5m, z=12.3m), and around $6.0 * 10^{-13}$ Rad/collision (1 kRad/10 LHC-years) at the top corner (x=4.0m, y=3.5m, z=12.3m). The dose values for ECAL in similar locations (x=0 and 4.0m, y=3.8m, z=12.5m) correspond to those of the Preshower within a 20% accuracy.

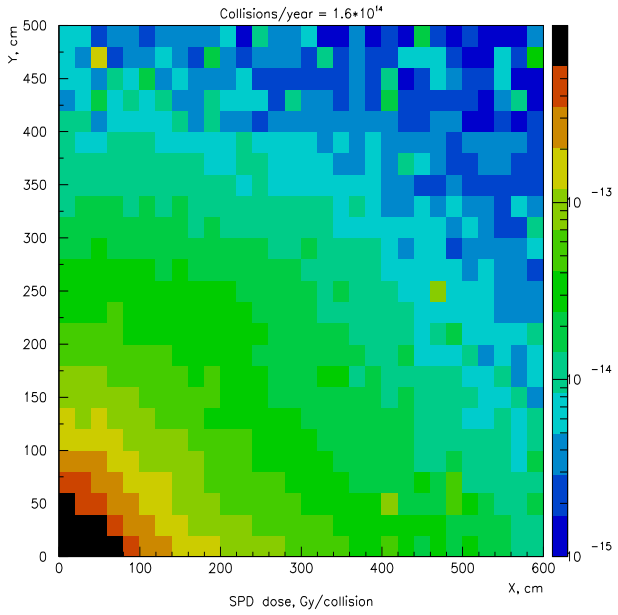

Figure 29: Dose in a plane upstream of the Preshower at $z = 1230$ cm

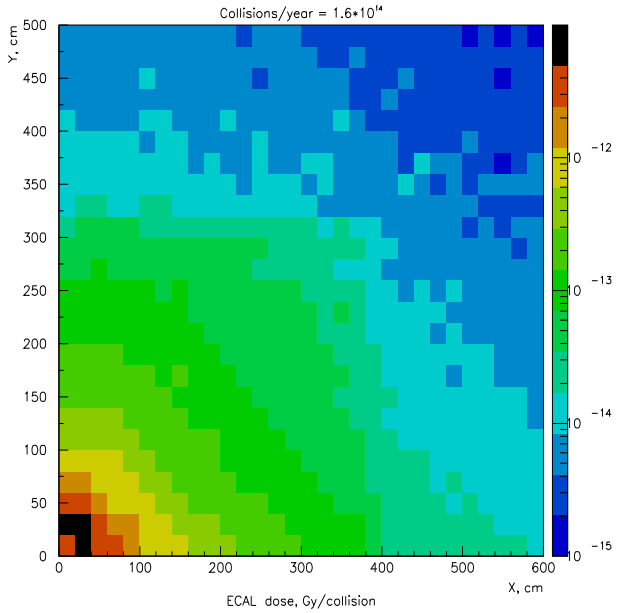

Figure 30: Dose in a plane upstream of ECAL at $z = 1250$ cm

3.4.2 Hadronic calorimeter.

Two different views of the details of the simulation model of the Hadronic calorimeter (HCAL) are shown in Fig.31 (y-z) and Fig. 32 (x-y). The little circles in the y-z view are to the channels for the calibrating radioactive sources while in the x-y view the steel and scintillating tyles, positioned parallel to the beam, are visible. The FLUKA model mimicks as closely as possible the structure of the detector [16].

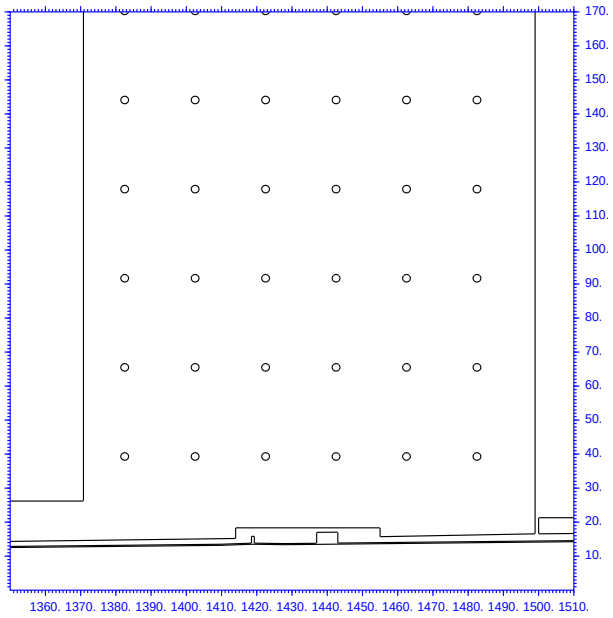

Figure 31: Detail of the HCAL simulation model (y-z cross section at $x = 5cm$)

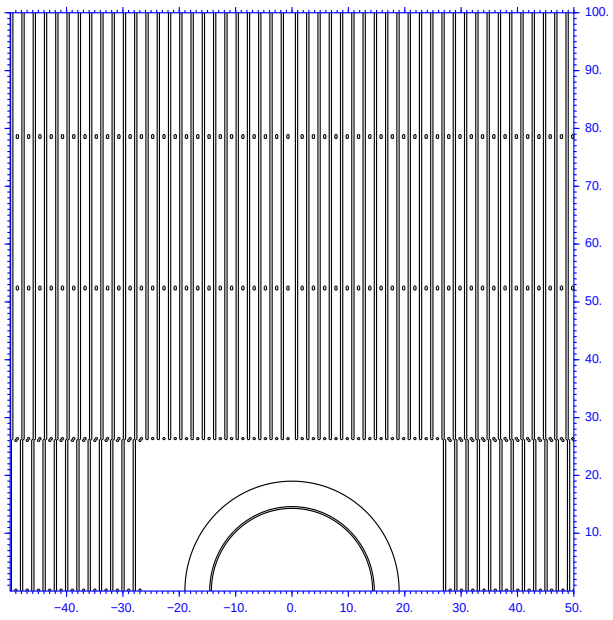

Figure 32: Detail of the HCAL simulation model (x-y cross section at $z = 1450cm$)

The dose map at the upstream surface of HCAL is shown in Fig.33. At the possible location of the HCAL electronics (on top the detector as for the Preshower and ECAL) the dose reaches $1.5 * 10^{-12}$ Rad/collision (2.4 kRad/10 LHC-years) at the center (x=0, y=3.8m, z=13.5) where it is higher, and $7.0*10^{-13}$ Rad/collision (1.1 kRad/10 LHC-years) in the corner (x=4.0m, y=3.8m, z=13.5m).

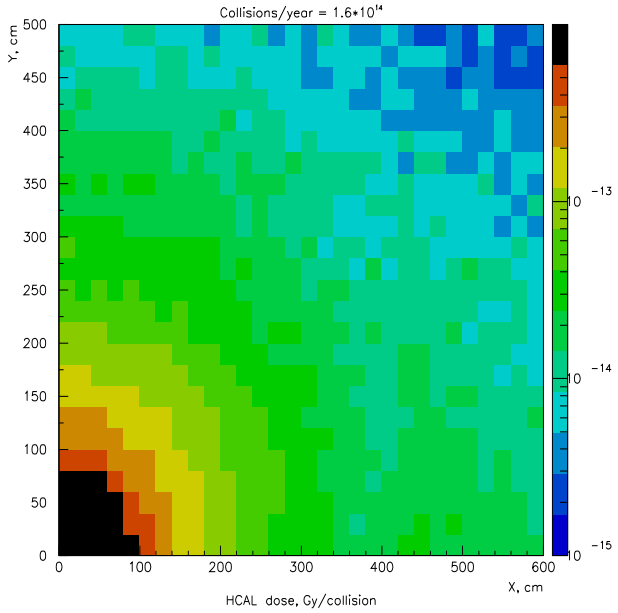

Figure 33: Dose at the upstream surface of HCAL ($z = 1350$cm)

3.5 Muon system

A simulation view of the muon system is shown in Fig.34, where the four downstream muon stations are interspersed with shielding walls of iron; each station is also protected by iron plugs surrounding the beam pipe. In the FLUKA simulation each muon station is described as a set of layers in z, reproducing the structure of the individual muon chambers [17]. No segmentation in x-y has been introduced and the frames of individual chambers have not been included. Muon station M1 is located upstream of the Calorimeters and not visible in this drawing.

The dose map obtained for one of the muon stations (M3) is shown in Fig. 35 as an example; it is strongly peaked toward the inner edges of the station. The effect of the shields on the radiation levels can be seen in the figure where the outer shape of the shield is visible, since the scoring plane extends beyond the station dimensions.

The electronics of the muon chambers will be distributed on the sides of each chamber. Since the chamber dimensions range from around $30\times25cm^2$ to $120\times25cm^2$ the electronics will be located all over the surface of a station. The maximum dose value is reached at the inner sides of a station. The maximum dose values for the four muon stations located in the shields are shown in Fig. 36

As mentioned before Muon station M1 is positioned upstream of the calorimeters, hence exposed to a much higher dose than the other muon stations. The dose map in

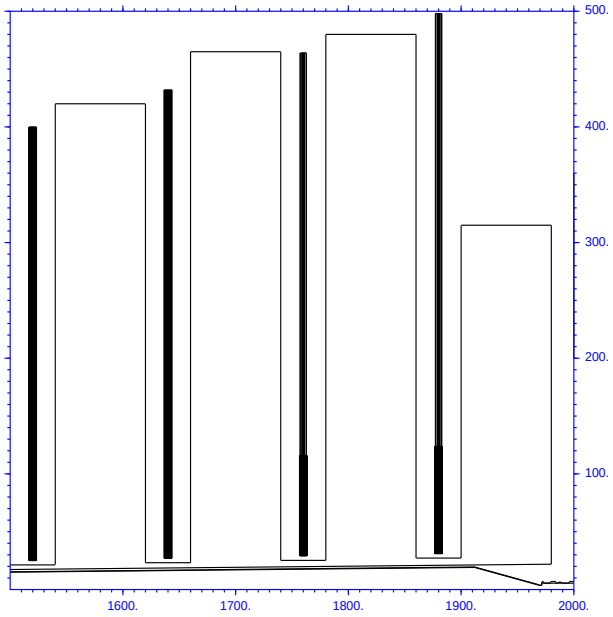

Figure 34: Cross section of the Muon stations 2-5 by $X = 0$ plane.

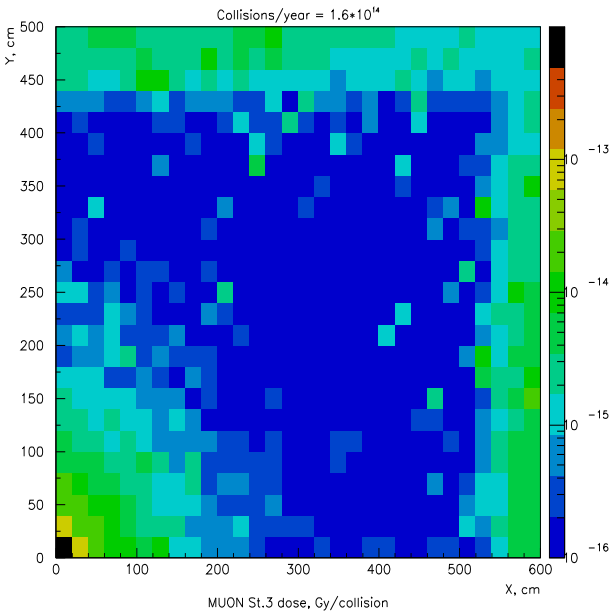

Figure 35: Dose in the middle plane of muon station M3 ($z = 16.4$ m)

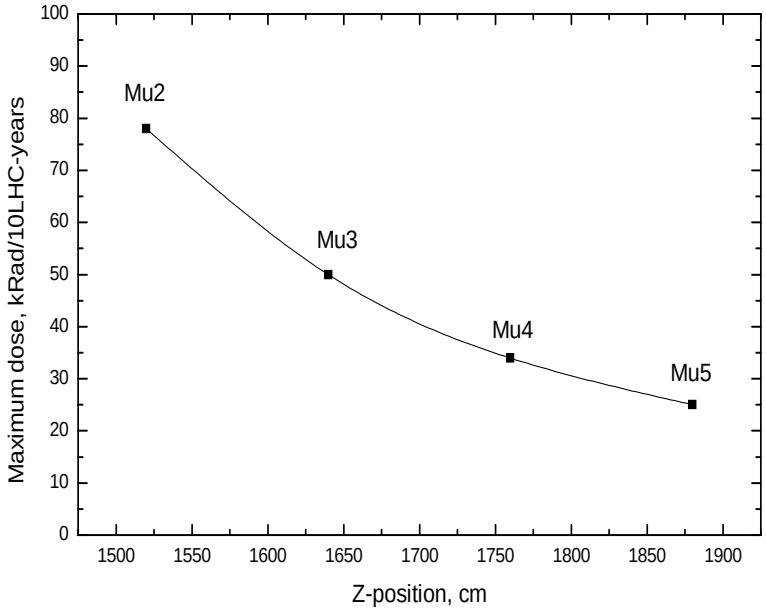

Figure 36: Maximum dose values in the middle planes of the Muon stations M2-M5

a scoring plane placed between the Preshower and M1 (z=1230cm) is shown in Fig. 29. The maximum dose at the inner edge of the station is close to $1.4 * 10^{-10}$ Rad/collision (230 kRad/10 LHC-years).

4 Summary

In this note we presented the summary of the results of a set of FLUKA simulations of the whole LHCb experimental setup [7]. Short comments on the geometry implementation of each subsystem as modelled in the simulation are given and values of doses and 1-MeV neutron equivalent fluence quoted for critical points. In Table 1 we summarize the dose and fluences for critical locations in different subsystems for 10 LHC-years.

Subsystem	Location (x,y,z) [cm, cm, cm]	Dose [kRad/10 LHC-years]	1 MeV n-eqv. fluence [n/cm^2/10 LHC-years]
VELO	Sensor (0.6, 0.1, 73)	50000	$2.4 * 10^{15}$
	Tank (60, 0, 70)	37	$2.0 * 10^{12}$
Trackers	TT inner edge (4, 0, 228)	4800	$4.8 * 10^{13}$
	T2, IT inner edge (9, 0, 852)	1000	$9 * 10^{12}$
	T2, OT outer edge (290, 0, 852)	2.1	-
RICH1	Photo-Detectors and electronics (0, 80, 160)	12	$1.7 * 10^{12}$
RICH2	Outer edge (400, 0, 1150)	4.3	-
PS/ECAL	Top edge (0, 350, 1230)	1.9	-
HCAL	Top edge (0, 380, 1350)	2.4	-
Muon System	M1 inner edge (30, 0, 1240)	230	-
	M3 inner edge (30, 0, 1640)	50	-
Cavern	Floor in concrete tunnel (0, -600, 1100)	0.06	-

Table 1: Summary of the dose and particle fluences in critical locations of different subsystems

References

[1] V.Talanov, Radiation environment at the LHCb vertex detector, LHCb-98-019

[2] V.Talanov, Estimation of absorbed dose levels at possible locations for LHCb detector, LHCb-2000-015

[3] V.Talanov, Radiation environment at the LHCb Inner Tracker area, LHCb-2000-013

[4] N.Sagidova GCALOR studies of background in the LHCb muon system, A.Tsaregorodtsev, A.Vorobyov, LHCb-98-059

[5] A.Tsaregorodtsev,Muon system parametrized background, LHCb-2000-011

[6] A.Fasso, A.Ferrari, J.Ranft, P.R.Sala., FLUKA: Status and Prospective for Hadronic applications, invited talk in the Proceedings of the Monte Carlo 2000 Conference, Lisbon, October 23-26, 2000, Springer-Verlag Berlin, p.955-960(2001)

[7] G.Corti and L.Shekhtman, Radiation studies with FLUKA, http://lhcb-background.web.cern.ch/lhcb-background/Radiation/RadLevels.htm

[8] The LHCb collaboration, Status of the LHCb detectro reoptimization, CERN/LHCC 2003-003

[9] J.Ranft, "DPMJET-II, a Dual Parton Model event generator for hadron-hadron, hadron-nuclus and nucleus-nucleus collisions", in Proc.of SARE2 workshop, CERN, October 9-11, 1995, CERN/TIS-RP/97-05

[10] A.Vasilescu and G.Lindstroem, Displacement damage in silicon, on-line compilation, http://sesam.desy.de/ gunnar/Si-dfunc.html

[11] VELO geometry optimization, T.Bowcock et.al, LHCb-2000-90

[12] O.Steinkamp, Layout of a cross-shaped Inner Tracker, LHCb-2001-114

[13] L.Shekhtman, Radiation background at the region of Inner Tracker, LHCb-2002-063.

[14] E.Gouchtchine et.al., Design and construction of the LHCb Scintillator-Pad/Preshower Detector, LHCb-2000-042.

[15] S.Barsuk et.al, Design and construction of the electromagnetic calorimeter for the LHCb experiment, LHCb-2000-043.

[16] R.Djeliadine et.al., The Hadron Calorimeter design and construction, LHCb-2000-045.

[17] P.R.Barbosa Marinho et al, LHCb Muon System Technical Design Report, CERN/LHCC 2001-010